Journal of Chromatography B, 911 (2012) 122–132

Contents lists available at SciVerse ScienceDirect

Journal of Chromatography B

journal homepage: www.elsevier.com/locate/chromb

Metabolism studies of benzbromarone in rats by high performance liquid chromatography–quadrupole time of flight mass spectrometry

Haiqing Wu[a,1], Ying Peng[a,*,1], Shaojie Wang[b], Kai Wang[a], Xunchen Zhao[c], Fan Jiang[a]

[a] Department of Pharmacy, Shenyang Pharmaceutical University, 103 Wen-Hua Road, Shenyang 110016, China
[b] Department of Medicinal Chemistry, Shenyang Pharmaceutical University, China
[c] Department of Natural Pharmaceutical Chemistry, Shenyang Pharmaceutical University, China

ARTICLE INFO

Article history:
Received 14 June 2012
Accepted 25 October 2012
Available online 2 November 2012

Keywords:
Benzbromarone
Metabolite
HPLC–QTOF-MS

ABSTRACT

A high performance liquid chromatography–quadrupole time of flight mass spectrometry (HPLC–QTOF-MS) method was employed in investigation of benzbromarone metabolites in rat plasma, urine, feces and bile samples. Meanwhile, the metabolic pathways of benzbromarone in rats were discussed. The identification was achieved on a reversed-phase C_{18} column with mobile phase gradient method. The QTOF-MS was operated under full scan of MS or MS/MS in negative mode. The fragments were acquired by raising collision induced dissociation (CID) energy for speculating the structures of parent ions. According to the information from the chromatograms and mass spectra, 17 metabolites were obtained. Among them, the deoxidized phase I metabolites and an array of phase II metabolites—sulfate conjugates detected in the biological samples made the work more significant.

1. Introduction

Gout is caused by high-level uric acid precipitation in the joints or soft tissues, causing joint pain, swelling and inflammation. Benzbromarone (BBR) is benzofuran derivative (as shown in Fig. 1) acting as an uricosuric agent by reducing the proximal tubular reabsorption of uric acid [1]. But recently, clinical cases of acute liver damage related to BBR [2–5] draw our attention to the metabolism profiles of BBR *in vivo*.

Debromination was considered to be a main bioactivation in the metabolic pathways of BBR *in vivo* before late 1980s [6,7]. It was clarified that hydroxylation rather than debromination was the predominant bioactivation of BBR in 1988 [8]. Soon after that, its metabolism study in a healthy volunteer was performed by Amold et al. [9], who determined six hydroxyl metabolites of BBR with comprehensive methods including HPLC, LC–MS and GC–MS. In addition, they pointed out that glucuronide conjugates were the major phase II metabolites with enzymatic hydrolysis method. In 1990s, many people held that the biotransformation of BBR varied in humans through a population study and that the toxicity of BBR might be a familial disorder [10–14]. The only data available on the toxicity of BBR in humans had been published by McDonald and Allan Rettic [1]. They insisted that a metabolite intermediate containing a catechol structure played a key role in its liver toxicity.

Although the metabolic properties of BBR have been examined, to date no systematic researches into its elimination *in vivo* have been presented with a fast and accurate analyzer. Therefore, it is important to develop sample preparation and analysis techniques for screening BBR metabolites in different biological matrices.

Recently, HPLC–QTOF has been proved a powerful and reliable analytical approach for *in vivo* metabolite identification studies. It is a combination of HPLC and QTOF technology for the identification of drug metabolites in biological matrices that adds a new dimension to metabolism studies enabling us to obtain better throughput, faster analysis, increased sensitivity, and increased peak resolution, which in turn will improve the data quality from the mass spectrometer [15,16].

Based upon the literature survey above, the present study aims to develop a rapid, simple and accurate approach to the comprehensive confirmation of BBR metabolites *in vivo* and meanwhile to lay the material foundation for further research on the BBR-induced hepatotoxicity from systematic studies on the plasma, urine, feces and bile samples of the oral dosed rats.

2. Experimental

2.1. Chemicals and reagents

BBR (>99.9% purity) was synthesized by ourselves; acetonitrile (HPLC grade, Fisher, USA); formic acid (HPLC grade, DIKMA, USA);

Abbreviations: HPLC–QTOF-MS, high performance liquid chromatography–quadrupole time of flight mass spectrometry; CID, collision induced dissociation; BBR, benzbromarone.

* Corresponding author. Tel.: +86 024 23986361; fax: +86 024 23986263.
E-mail address: yingpeng1999@gmail.com (Y. Peng).

[1] These authors made equal contribution to the article.

1570-0232/$ – see front matter © 2012 Elsevier B.V. All rights reserved.
http://dx.doi.org/10.1016/j.jchromb.2012.10.035

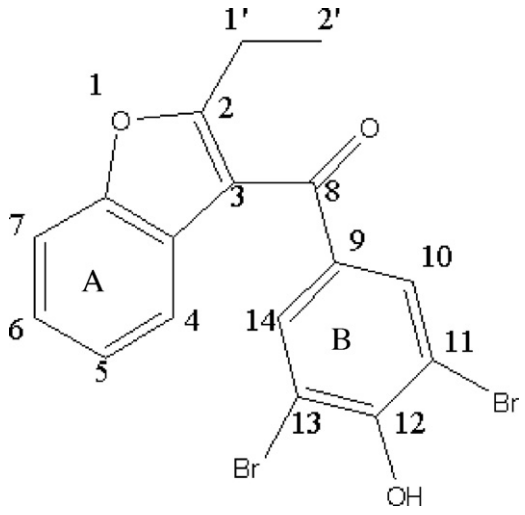

Fig. 1. The structure of BBR.

Table 1
Gradient of mobile phase for separation.

t (min)	Phase A (%)	Phase B (%)
0	20	80
20	60	40
30	90	10
35	20	80

Note: *Note:* Phase A: acetonitrile with 0.2% formic acid; Phase B: water with 0.2% formic acid.

other solvents were purchased commercially with purity of analytical or HPLC grade.

2.2. Instrumentations

HPLC system (Agilent, USA) consisted of a model G1276A pump, model G1367B autosampler and model G1316A UV-detector. The chromatograph was equipped with a reversed-phase C_{18} column of Waters (4.6 mm × 75 mm, 3.5 μm, USA) eluted with a gradient mobile phase (tabulated in Table 1). The flow rate was 0.8 mL min^{-1} and the column temperature was ambient temperature. The UV detector was set at 235 nm. An accurate splitter was used to split the flow into 1:3 before introduction into MS.

The QTOF-MS system (Bruker, Germany) with an ESI source was performed in negative mode. The parameters of ESI-MS were set as follows: capillary voltage (+3800 V), the nebulizer gas pressure (1.2 bar), the dry gas flow rate (8.0 L min^{-1}) and temperature (180 °C). MS conditions were corrected by direct infusion of sodium formic acid solution (1 mM L^{-1}) delivered by a syringe pump at a flow rate of 3 μL min^{-1}. The data were analyzed by Bruker Daltonics Data Analysis 3.4 software.

2.3. Animal handling and sample collection

The investigations were performed on nine male Sprague–Dawley rats (220 ± 20 g) provided by the Department of Experimental Animals of Shenyang Pharmaceutical University (Shenyang, China). Environmental controls for the animal room were set as follows: temperature at 22 ± 3 °C, relative humidity at 55 ± 5%, and a 12-h light/dark cycle. The animal studies were approved by the Animal Ethics Committee of Shenyang Pharmaceutical University and carried out in accordance with the requirements of Chinese national legislation.

The rats were fasted for 12 h prior to the study and allowed water *ad libitum*. The rats were exposed to BBR (25 mg kg^{-1} bodyweight) prepared with 0.5% sodium carboxymethyl cellulose solution (2.0 mg mL^{-1}) for a common oral dosing, and then fasted with free access to water.

2.3.1. Plasma sample collection

The blood samples at each time point were collected from three of rats. The samples were respectively collected from the eye bottom into heparinized tubes at the predose, 2, 4, 6, 8, 10 and 12 h after the dosing for about 0.3 mL each time. Each sample was centrifuged at 1650 × *g* for 10 min. The plasma obtained after the dosing was mixed, and all plasma was stored at −20 °C until analyzed.

2.3.2. Urine and feces sample collection

Three of rats had been housed individually in metabolic cages for a week and allowed access to water and food freely. The urine and feces samples were both collected for 24 h before and after the dosing, respectively. The urine sample was centrifuged at 1650 × *g*

Table 2
All the metabolites detected after an oral administration of BBR (25 mg kg^{-1}) to rats.

Phase[a]	No.	t_R (min)	[M−H]$^-$				Source[b]	Compound presumed
			Calculated	Detected	Error (ppm)	Sigma		
P	0	25.5	420.9080	420.9059	−5.7	0.009	p, u, f, b	$C_{17}H_{12}Br_2O_3$
I	1[c]	7.1	470.9084	470.9084	0.0	0.029	p, u	$C_{17}H_{14}Br_2O_6$
I	2[c]	11.2	454.9135	454.9100	−8.2	0.017	p, f, u	$C_{17}H_{14}Br_2O_5$
I	3	11.7	498.8940	498.8894	−9.2	0.023	u	$C_{18}H_{14}Br_2O_7$
I	4	12.9	452.8979	452.8946	−5.5	0.013	p, u, f, b	$C_{17}H_{12}Br_2O_5$
I	5	16.7	436.9030	436.9025	−3.4	0.029	p, u, f, b	$C_{17}H_{12}Br_2O_4$
I	6	18.1	436.9030	436.9014	−2.4	0.010	p, u, f, b	$C_{17}H_{12}Br_2O_4$
I	7	18.9	436.9030	436.9036	1.9	0.041	p, u, f, b	$C_{17}H_{12}Br_2O_4$
II	8	6.5	628.9300	628.9279	−3.2	0.008	b	$C_{23}H_{20}Br_2O_{11}$
II	9	6.9	628.9300	628.9277	−3.0	0.008	b	$C_{23}H_{20}Br_2O_{11}$
II	10	8.3	628.9300	628.9292	−0.2	0.009	u, b	$C_{23}H_{20}Br_2O_{11}$
II	11	10.2	612.9350	612.9395	7.1	0.011	b	$C_{23}H_{20}Br_2O_{10}$
II	12	11.0	612.9350	612.9389	5.3	0.019	b	$C_{23}H_{20}Br_2O_{10}$
II	13	12.0	612.9350	612.9374	3.4	0.016	u, b	$C_{23}H_{20}Br_2O_{10}$
II	14	14.5	514.8441	514.8492	9.9	0.037	u	$C_{17}H_{10}Br_2O_7S$
II	15	17.5	498.8492	498.8527	7.0	0.046	p, f, u	$C_{17}H_{10}Br_2O_6S$
II	16	23.5	532.8547	532.8593	8.6	0.018	u, b	$C_{17}H_{12}Br_2O_8S$
II	17	26.5	516.8598	516.8569	−5.7	0.018	u	$C_{17}H_{12}Br_2O_7S$

[a] Phase: p, parent drug; I, phase I metabolite; II, phase II metabolite.
[b] Source: p, plasma; u, urine; f, feces; b, bile.
[c] The reduced metabolites.

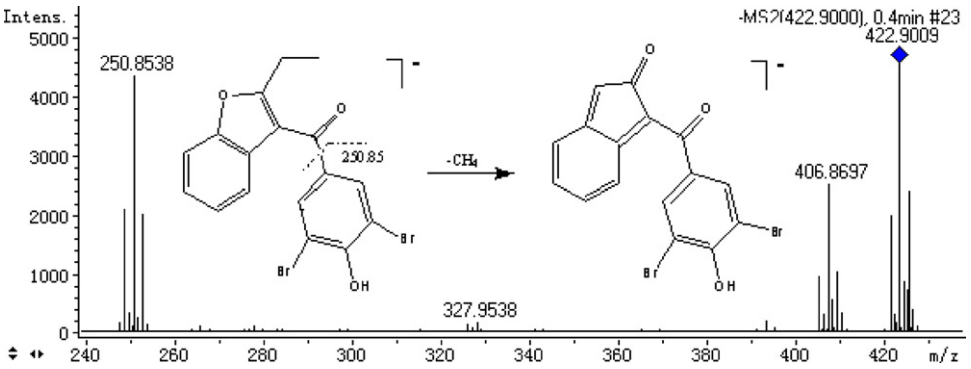

Fig. 2. MS/MS spectrum of $[M+2-H]^-$ of M0 and its fragmentation pathways.

for 10 min and the supernatant was stored at −20 °C until analyzed. The feces was left in a cool and dry place to dryness.

2.3.3. Bile sample collection

Three of rats were used for bile duct intubation. They were anesthestized with ether followed by the collection of blank bile samples. Then they were dosed with BBR (25 mg kg^{-1}) after they were awake. The bile samples were respectively collected at 0–2, 2–4, 4–6, 6–8, 8–10 and 10–12 h after the dosing, and the rats were anesthetized with ketamine–acepromazine (50:3.3 mg kg^{-1}) solution in the process. All samples were stored at −20 °C until analyzed.

2.4. Sample preparation

2.4.1. The extraction pretreatment of plasma, urine and bile samples

Each sample was extracted by ethyl acetate. 400 μL of each sample was mixed with 80-μL volume of hydrochloric acid solution (1 mol L^{-1}) and ethyl acetate (1.2 mL). The resultant mixture was vortexed for 3 min and centrifugated at 6650 × *g* for 10 min. The upper organic layer was transferred and evaporated to dryness under a stream of nitrogen gas at 40 °C. The residue was reconstituted by 100 μL of the initial mobile phase, and 20 μL was injected into the HPLC–QTOF-MS system.

2.4.2. The precipitation pretreatment of urine samples

For urine samples, another aliquot was processed by precipitation. 400 μL of each sample was mixed with 1 mL of acetonitrile, then the resultant mixture was vortexed for 3 min, and the rest steps followed in Section 2.4.1.

2.4.3. The pretreatment of feces samples

Half of the total weight of each feces sample was extracted with methanol (200 mg: 1 mL) by ultrasound for 10 min and centrifuged at 6650 × *g* for 10 min. 400 μL of the

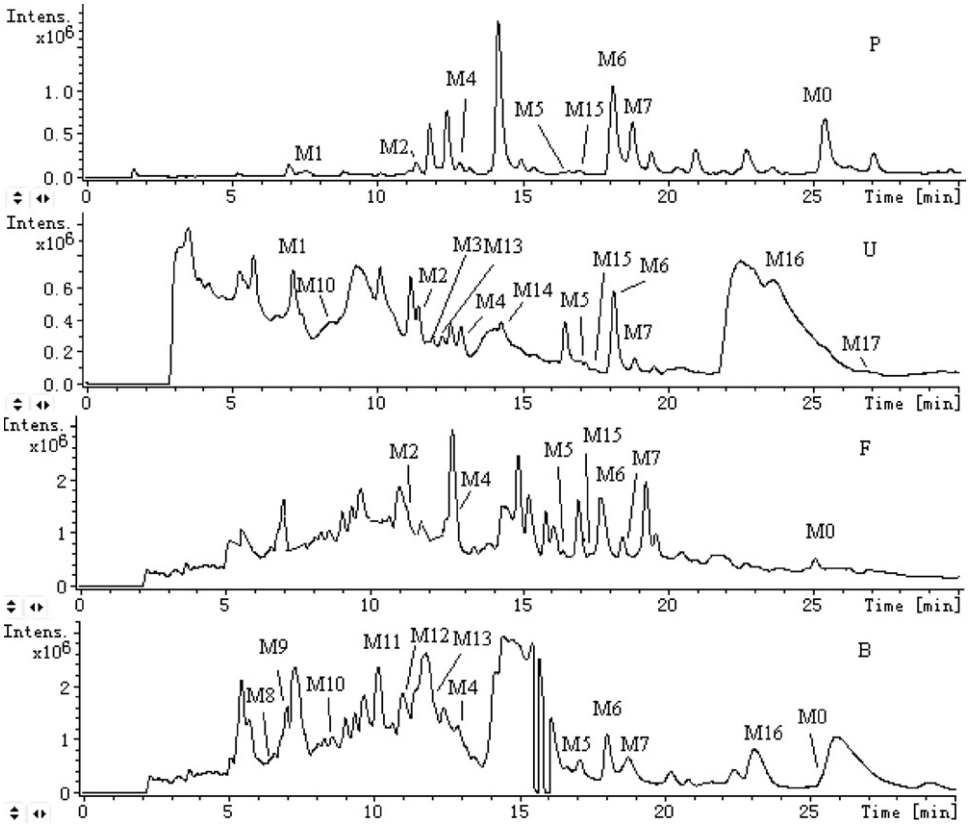

Fig. 3. TIC (total ion chromatograms) of extracted plasma (P), feces (F), bile (B) samples and the precipitated urine (U) samples of rats after an oral administration of BBR (25 mg kg^{-1}) analyzed by HPLC–QTOF-MS.

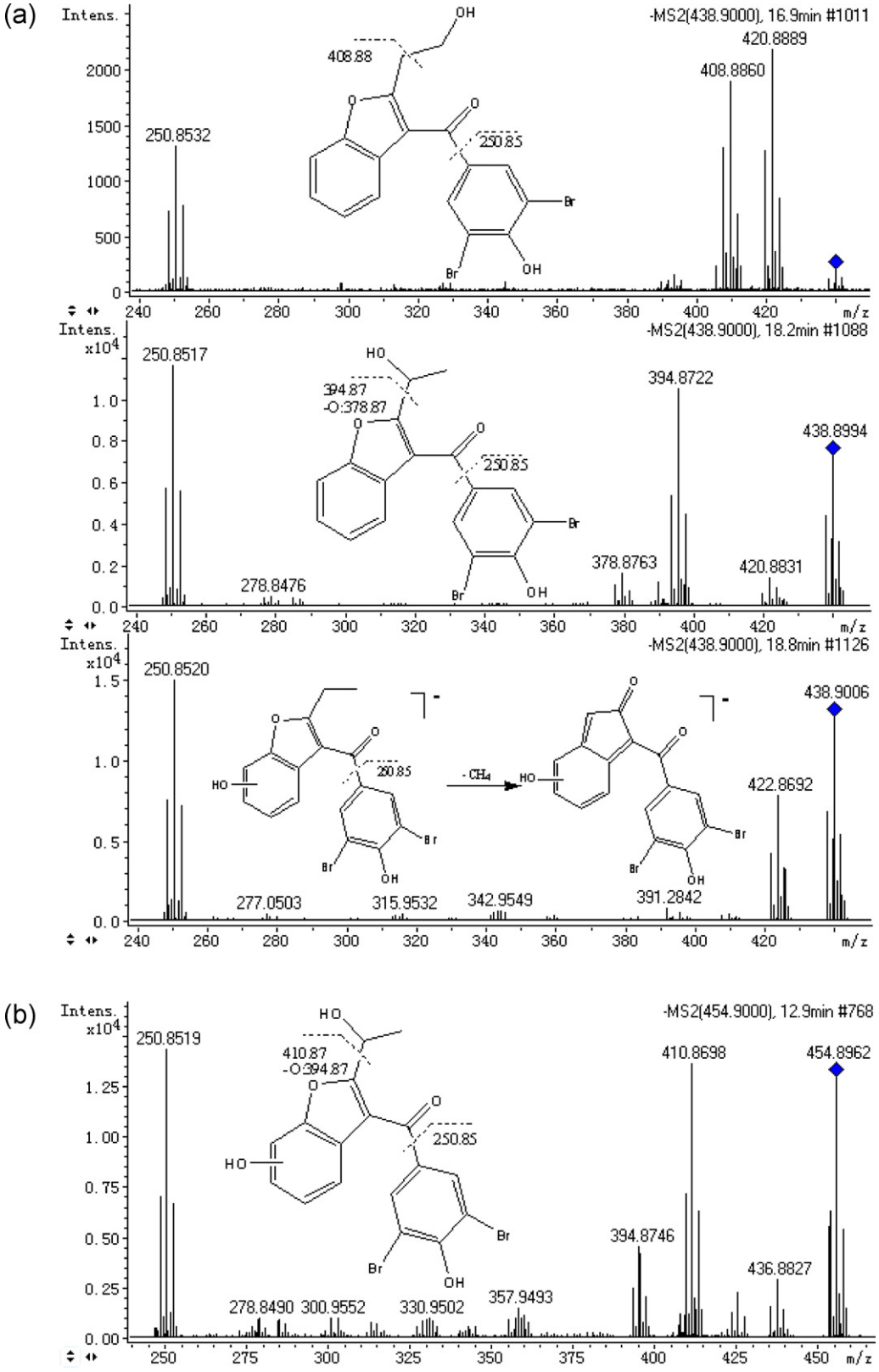

Fig. 4. (a) MS/MS spectra of $[M+2-H]^-$ of M5, M6, M7 and their fragmentation pathways, (b) MS/MS spectrum of $[M+2-H]^-$ of M4 and its fragmentation pathways, (c) MS/MS spectrum of $[M+2-H]^-$ of M2 and its fragmentation pathways, (d) MS/MS spectrum of $[M+2-H]^-$ of M1 and its fragmentation pathways and (e) MS/MS spectrum of $[M+2-H]^-$ of M3 and its fragmentation pathways.

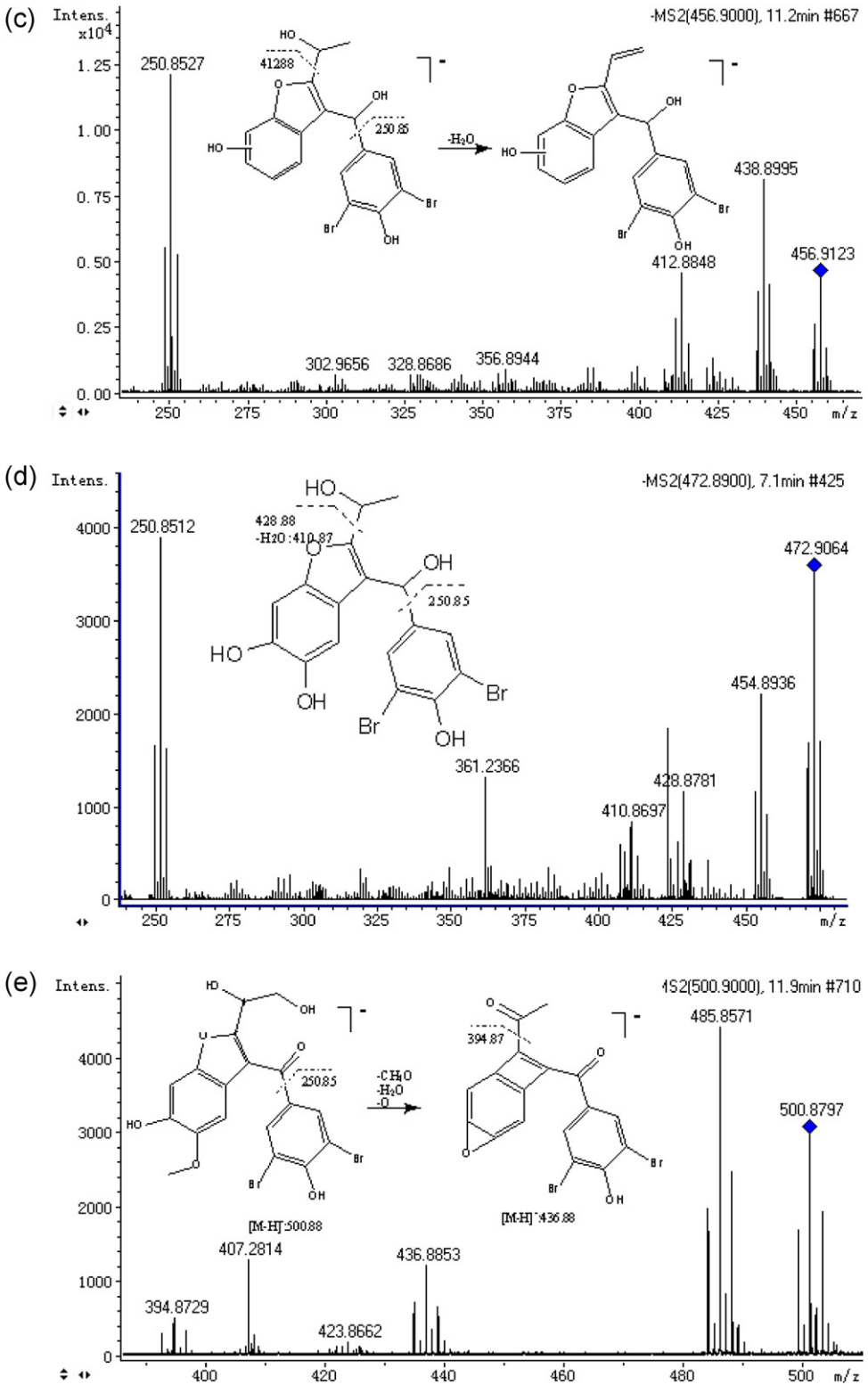

Fig. 4. (a)(*Continued*)

supernatant was used, and the rest steps followed in Section 2.4.1.

3. Results and discussion

The MS spectra were obtained in negative mode using HPLC–QTOF-MS, and the experimental conditions were optimized as follows.

3.1. Optimization of sample pretreatment

Initially, we handled all samples with extraction and precipitation in accordance with the literature methods [17]. For plasma and feces samples, the metabolite species did not show marked difference in extracted samples from those in precipitated samples. Allowing for the relative resolution and background noise, the plasma and feces samples were achieved by extraction with

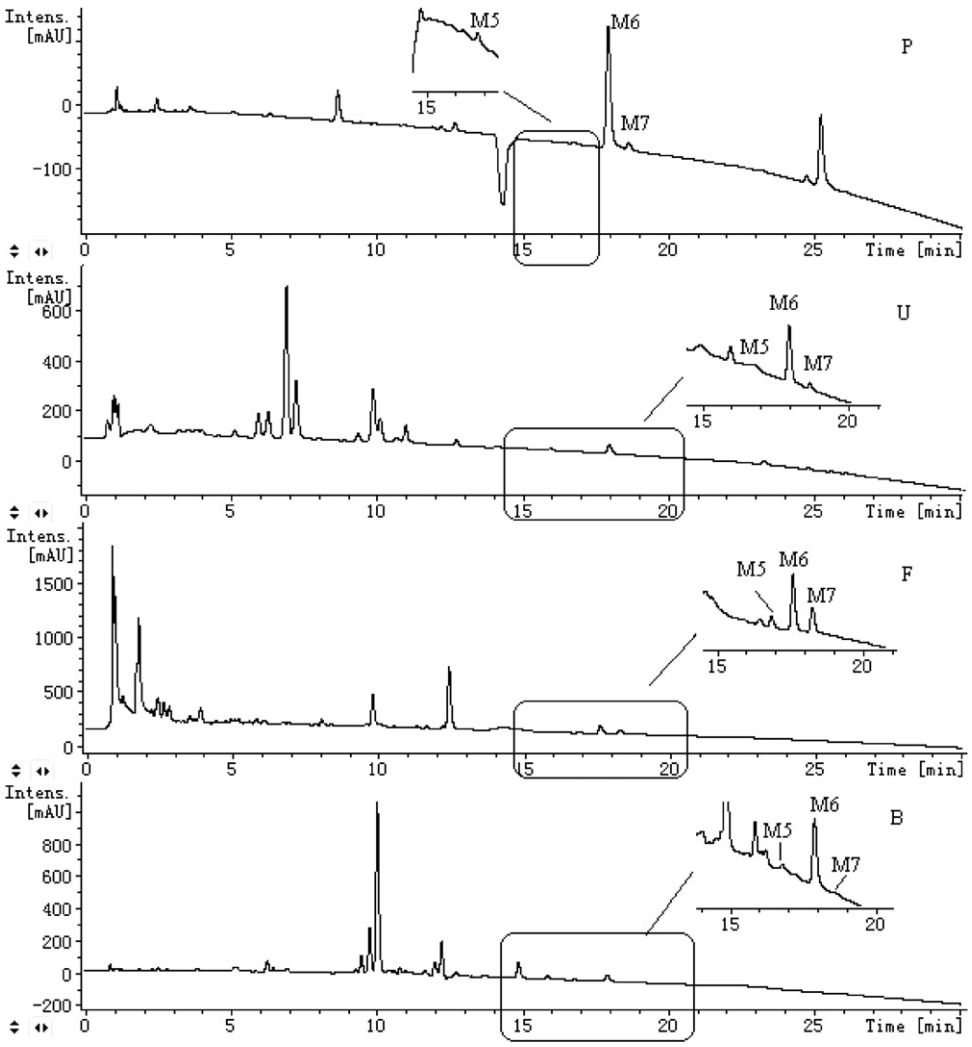

Fig. 5. The UV Chromatograms of four biological samples (P: plasma; U: urine; F: fences; B: bile) analyzed by HPLC–QTOF-MS.

ethyl acetate. In the precipitated urine samples, there were more phase II metabolites than those in the extracted urine samples. Thus, we chose the precipitated urine samples for analysis of phase II metabolites and the extracted urine samples for phase I metabolites in consideration of good separation of phase I metabolites from interference in extracted samples. Owing to the unacceptable background noise in precipitated blank bile samples, we treated bile samples by means of extraction.

In previous studies [18,19], enzymatic hydrolysis or acidic hydrolysis method was traditionally employed in detection of phase II metabolites. Here, application of direct precipitation in order not to overlook all conjugated metabolites, while somewhat unconventional, was proven to be a simple, economic and feasible method for research into phase II metabolites. In this way, a series of sulfate adducts were surprisingly obtained.

3.2. The optimization of chromatographic separation

The optimization of LC conditions was focused on improving the shape of peaks in order to achieve good separation among major substances from complicated matrices. Triethylamine was a first choice as a modifier to avoid tailing. However, it could have ion suppression effect on the compounds of interest because of its good ionization. Irrespective of sulfate adducts, which still gave bad tailing peaks, we chose 0.2% formic acid as the modifier in spite of scanning in negative mode.

3.3. The optimization of MS and MS/MS condition

In our study, the negative ion mode was advantageous over the positive mode for detection of quasi molecular ions. The main reasons were that quasi molecular ions appeared in $[M+H]^+$ and $[M+Na]^+$ in positive mode, which brought about decline of peak intensity, and the instability of $[M+Na]^+$ made it not fit for MS/MS analysis.

The optimization of MS/MS conditions was focused on the optimization of CID energy to obtain abundant fragments for structure analysis. We found that all metabolites would produce abundant fragments when CID energy was between 15 eV and 30 eV. Besides, phase II metabolites tended to eliminate the neutral fractions, so the CID energy could be lower. In fact, for most phase II metabolites, the cleavage could happen even in the MS mode.

3.4. The analysis of mass spectra

In the study, the particular attention was concentrated on analyzing every spectrum of each metabolite and speculating possible metabolism pathways of BBR in rats. The metabolites were predicted with a high degree of confidence. If a peak appeared from

the accurate extracted ion chromatograms (EIC) in the experimental group and the accurately measured mass in the MS spectrum agreed with the theoretical mass within 10 ppm based on the predicted formula, then the peak was proposed as the metabolite. If the peak was absent from the accurate EIC in the experimental group, the metabolite was not formed. Fortunately, the typical patterns of two bromine atoms isotope (1:2:1) made the work more reliable and uncomplicated. Additionally, the Sigma value (<0.05) gave by the workstation that characterizes the degree of the isotope matching made the data reliable. And then, the elemental composition of a metabolite was speculated in two steps. In the first step, the quasi molecular ion mass of each metabolite was compared with that of BBR to provide a preliminary indication of the metabolite; in the following step, postulated structure of the metabolite was deduced from the fragments detected in the ESI mode. So these fragment ions were used as references to aid in interpretation of the product ions of the metabolites, as well as to examine the high resolution and mass accuracy of the instrument. However, the information of mass spectrometry alone was not always sufficient for identifying the site of biotransformation, the retention behavior was involved.

A total of 17 metabolites (as shown in Fig. 3 and summarized in Table 2) from four biological samples were characterized based on their retention behaviors and MS spectra. The investigated metabolite was sequenced according to HPLC retention time and phase of the metabolite, but interpretation of every metabolite was done according to the possible metabolic process sequence.

3.4.1. The parent drug—M0

As shown in Fig. 2, authentic BBR was characterized by signal of $[M+2-H]^-$ ion at *m/z* 422.9009 *via* direct injection. The fragment ion at *m/z* 406.8697 was formed by loss of CH_4 (predicted 406.8747 Da) rather than O (predicted 406.9112 Da) from M0 and rearrangement reaction, which could be differentiated only with a high-resolution instrument. The other important fragment ion at *m/z* 250.8538 was used for monitoring the unchanged ring B in the paper below. According the obtained results, the fragmentation pathways of M0 were proposed in Fig. 2.

3.4.2. Phase I metabolites

Seven phase I metabolites were obtained and all of them were detectable in urine sample (as shown in Fig. 3).

MS spectra of M5 (t_R 16.7 min), M6 (t_R 18.1 min) and M7 (t_R 18.9 min) illustrated the same $[M+2-H]^-$ ions at *m/z* 438.90 which

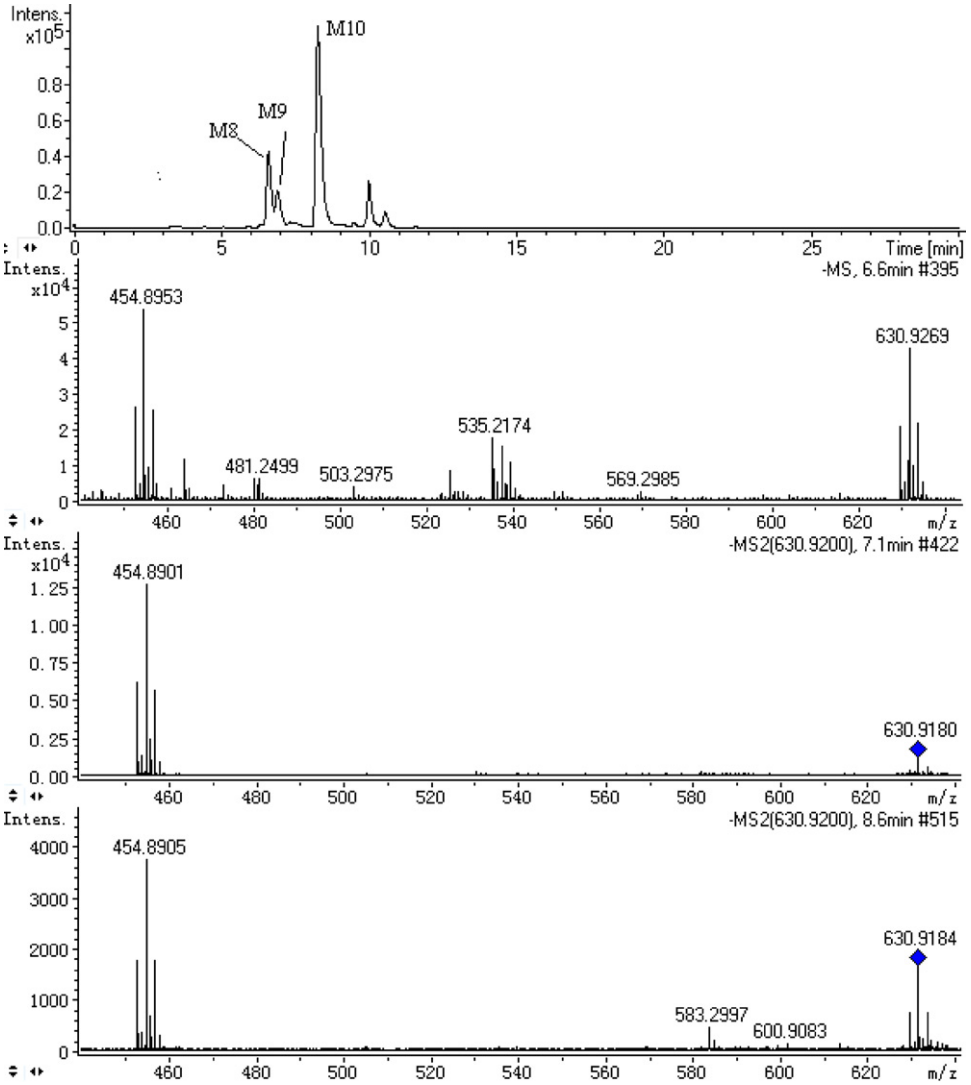

Fig. 6. (a) EIC (extracted ion chromatograms) of $[M+2-H]^-$ ion of *m/z* at 630.92 and fragmentation of M8–M10 in ion source or in MS/MS mode, (b) EIC (extracted ion chromatograms) of $[M+2-H]^-$ ion of *m/z* at 614.93 and fragmentation of M11–M13 in ion source or in MS/MS mode and (c) fragmentation of M14–M17 in ion source or in MS/MS mode.

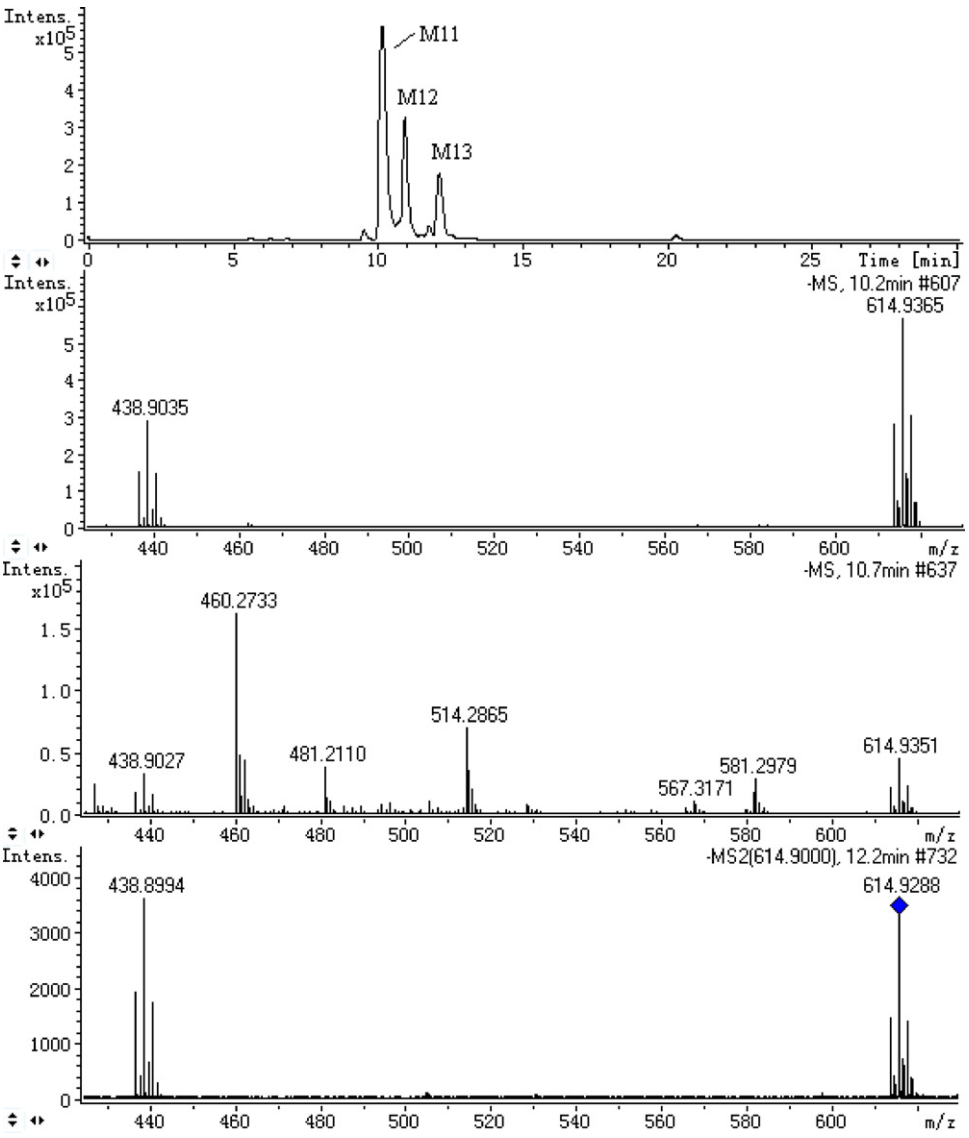

Fig. 6. (b) (*Continued*)

was 16 Da higher than that of BBR due to the additional substitution of a hydroxyl group.

3.4.2.1. Identification of M5. According to the fragment ion at *m/z* 408.8860 (loss of CH_2O) and *m/z* 420.8889 (elimination of H_2O) given in Fig. 4a, the structure of M5 could be assigned to the OH substituent in C-2′.

3.4.2.2. Identification of M6. The fragment ion at *m/z* 394.8722 corresponded to loss of C_2H_4O (*m/z* 44.0268) from M6, which gave us the information that the hydroxylation of BBR was in the side chain, and the fragmentation pathways of hydroxylation of BBR in C-2′ had been described above, and hydroxylation site in M6 should be in C-1′. Comparing the MS/MS spectra of M5 and M6 in Fig. 4a, it was concluded that the presence of OH group on C-l′ in M6 induced to the well-defined loss of side chain and the presence of OH group on C-2′ in M5 generated the typical fragment by loss of CH_2O.

3.4.2.3. Identification of M7. As described above, if BBR had undergone hydroxylation on either carbon (1′ or 2′) of the ethyl moiety, we would have expected to see significant fragmentation peaks at $[M+2-H]^- - 18$ (*m/z* 420.88) in the MS/MS mode, due to the loss of water. Therefore, the absence of fragments from loss of water could serve as differentiation between M7 and M5 with M6, and M7 should be formed by hydroxylation on ring A or ring B. The OH group on ring B was excluded by the hint of fragment ion at *m/z* 250.8520. Nevertheless, the exact position of the OH group on ring A could hardly be elucidated by means of LC–MS. The fragment ion at *m/z* 422.8692 was assigned to loss of methane in the similar fragmentation pathway to that of M0.

It could be concluded from Fig. 5 that the hydroxylation on C-l′ was more favored, because it was found in the largest excess among the three of one hydroxylation metabolites in all biological samples.

Relative intensity of UV chromatographic peak of M7 was much lower than that of M6 but higher than that of M5 in plasma, urine and bile samples. Interestingly, its intensity was much higher in feces samples than in the other samples.

3.4.2.4. Identification of M4. The CID spectrum of M4 (t_R 12.9 min) was depicted in Fig. 4b. The presence of $[M+2-H]^-$ ion at *m/z* 454.8962 provided evidence of the additional substitutions of two hydroxyl groups. This compound was found to have similar fragmentation pathway (410.8698 $[M+2-C_2H_4O-H]^-$) to that of M6, which demonstrated that one OH group was located in C-1′ at

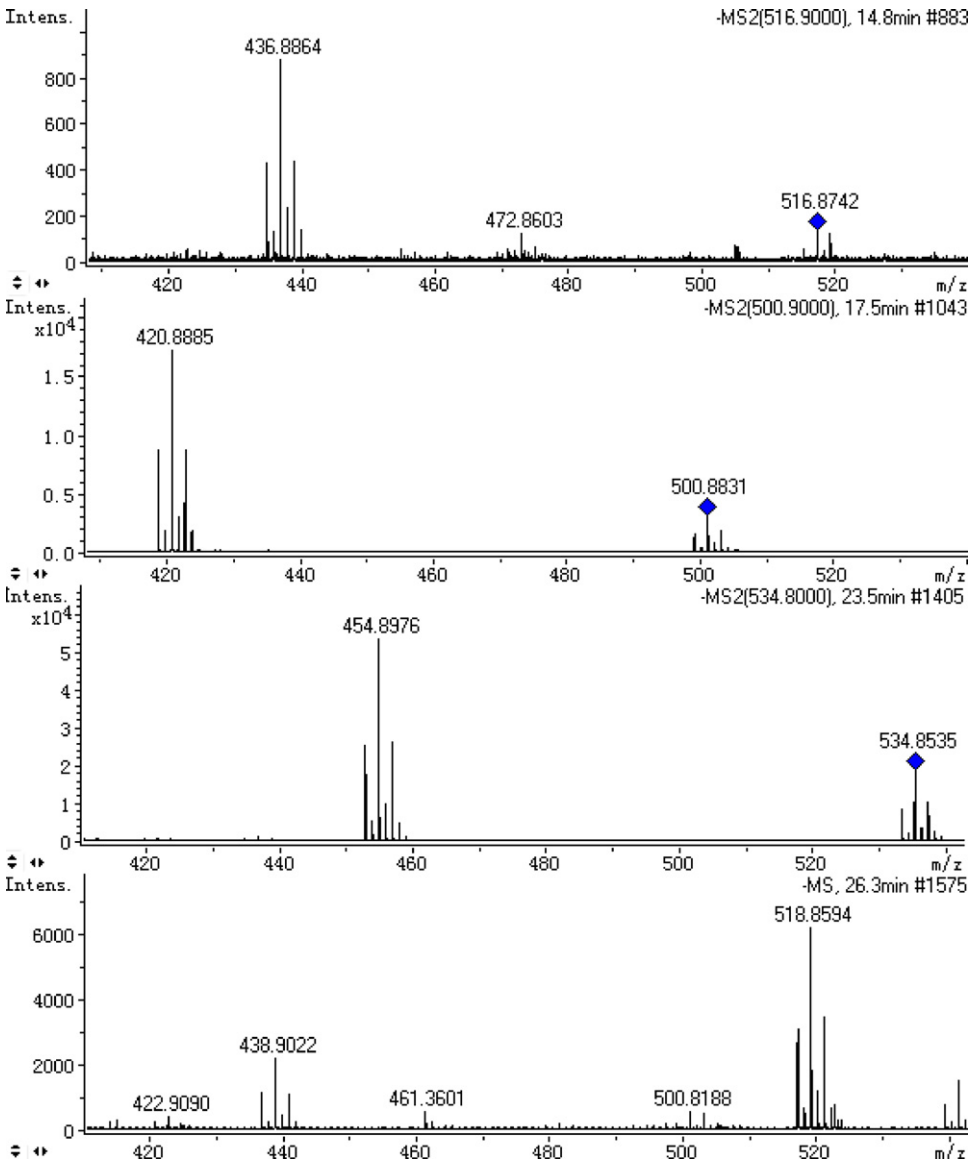

Fig. 6. (c) (*Continued*)

the side chain. The relative low abundance of fragment ion at *m/z* 424.8848 (loss of CH_2O) proved that the OH group at the side chain could be located in C-2′ in trace. Because of similar polarity and the absolutely same mass of parent ions, distinction of the two compounds could hardly be achieved from the information of LC and MS analysis, but their fragments in MS/MS mode gave us the difference between the two metabolites. The fragment ion at *m/z* 250.8519 was used for monitoring the unchanged ring B as noted above, thereby, the second OH group was finally considered to be located in ring A. Furthermore, the fragment ion at *m/z* 436.8827 was generated by elimination of water from the side chain, which verified the conclusion above. The absolute same mass number of the fragment at *m/z* 394.8746 as that produced by M7 illustrated that two of the fragments should have the same elemental composition, and it was speculated that the fragment should be produced by loss of an oxygen atom (*m/z* 15.9955) from the fragment ion at *m/z* 410.8698. But loss of oxygen atom was no more favorable from the hydroxyl group already attached to the adjacent carbon atom of double bond (or aromatic ring). Therefore, the loss must be in the fragmentation pathway as illustrated in Fig. 4b.

3.4.2.5. Identification of M2. As illustrated in Fig. 4c, $[M+2-H]^-$ ion at *m/z* 456.9123 was 2 Da higher than that of M4 (454.8962), suggesting that M2 might be the reduction derivative of M4. The possible reduced group might be the double bond between C-2 and C-3 or the only carbonyl. By comparison of retention behaviors of M2 (t_R 11.2 min) and M4 (t_R 12.9 min), it was found that the difference in polarity between M2 and M4 was apparent, which should be the contribution of conversion of carbonyl into alcohol, but not the ethilenic bond into saturated bond. Therefore, the structure of M2 was tentatively identified and its fragment pathways were explained in Fig. 4c.

3.4.2.6. Identification of M1. A possible metabolite—M1 was observed at 7.1 min with a quasi molecular $[M+2-H]^-$ ion at *m/z* 472.9064 which was 16 Da higher than that of M2 (456.9123) due to the additional substitution of a hydroxyl group. This compound was found to have similar cleavage pathways ($[M+2-H_2O-H]^-$ ion at *m/z* 454.8936 and $[M+2-C_2H_4O-H]^-$ ion at *m/z* 428.8781) to those of M2, which referred a hydroxyl radical existed in the side chain, more precisely, the OH group should be in C-1′, in according to the absence of the fragment by loss of CH_2O and presence of the

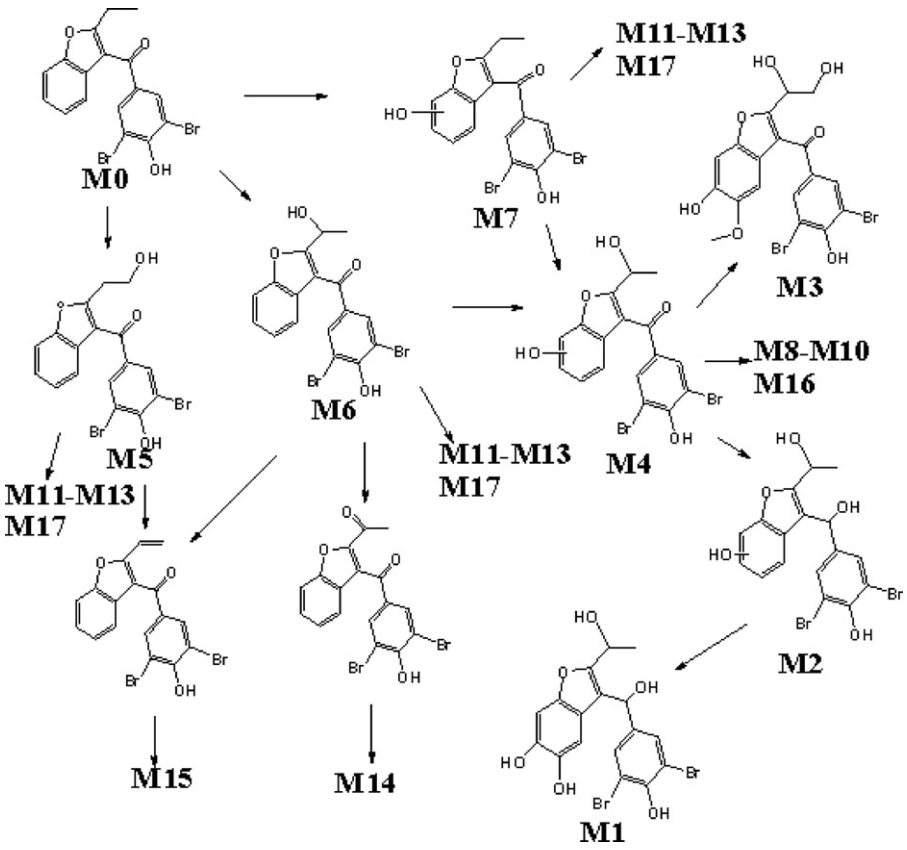

Fig. 7. Proposed *in vivo* metabolic pathways of BBR in rats.

fragment by elimination of C_2H_4O. Therefore, we concluded the OH group to be determined should be on ring A or ring B. Evidently, there was no change on ring B corroborated by fragment ion at *m/z* 250.8512, alternatively, and the OH group was beyond all doubt in the ring A. Moreover, the fragment ion at *m/z* 410.8697 was generated by the fragment ion at *m/z* 428.8781 through further loss of water, and hence, the two OH groups on ring A unequivocally formed into an *o*-phenol structure. The fragmentation pathways of M1 were proposed in Fig. 4d (the two OH groups on ring A were drawn in C-5 and C-6 for convenience of interpretation).

3.4.2.7. Identification of M3. The MS/MS spectrum of M3 was depicted in Fig. 4e. M3 (t_R 11.7 min) generated $[M+2-H]^-$ ion at *m/z* 500.8805 which underwent α-cleavage with elimination of a $^{\bullet}CH_3$ to generate the dominating fragment ion at *m/z* 485.8577 in spite of the loss 'violating' the even-electron rule. By comparison of $[M+2-H]^-$ of M3 and M1, M3 was suspected to be the methylated metabolite of M1. The postulated methylated structure would be in two patterns based on the information of *m/z* 500.8805. One was methylation of M1 for two times; the other would be methylation of M1 for one time, but the carbonyl still existed and another OH group was added. Nevertheless, the former was excluded by the accurate mass (the calculated mass of the former $[M-H]^-$ ion at *m/z* 498.9397, and that of the latter at *m/z* 498.8940). In supporting the present speculation, Isorhamnetin standard, a guaigcol derivative, was employed as a reference in MS and MS/MS through direct injection due to its close structure to the hypothesized compound. The exciting result testified that *o*-methoxyphenol could be identified by loss of the methyl group to generate an odd electron ion and neutral loss of CH_4O to form a heterocycle structure in negative mode, showing agreement with our supposition. The tentative identification of M3 was done as shown in Fig. 4e (the two OH groups on ring A were drawn in C-5 and C-6 for the convenience of interpretation).

3.4.3. Phase II metabolites

3.4.3.1. Glucuronide conjugates. As shown in Fig. 6a and b, M8 (t_R 6.5 min), M9 (t_R 6.9 min), M10 (t_R 8.3 min) generated $[M+2-H]^-$ ion at *m/z* 630.92, and M11 (t_R 10.2 min) M12 (t_R 11.0 min), M13 (t_R 12.0 min) at *m/z* 614.93. In ion source or in MS/MS mode, M8–M12 were observed to lose the same neutral molecule $C_6H_8O_6$ (176) and produce phase I metabolites.

The difference in retention behaviors of the same *m/z* adducts was in correlation with the different phase I metabolites or the different positions of OH group on the same metabolite combined with glucuronic acid.

3.4.3.2. Sulfate conjugates. As shown in Fig. 6c, the same loss of neutral molecule SO_3 (80) from M14 (t_R 14.5 min), M15 (t_R 17.5 min), M16 (t_R 23.5 min) and M17 (t_R 26.5 min) was observed in MS or MS/MS mode, thus, they were believed to be the sulfate adducts of the phase I metabolites known or unknown.

According to the present results, BBR was found to undergo hydroxylation metabolism as the predominant route to elimination, and hydroxylation positions were mainly on C-1′ and benzofuran. Further hydroxylation would continue on the initial metabolites to form multi-hydroxylation metabolites, and the major phase I metabolites could combine with glucuronide or sulfate in varying degrees. The possible metabolic pathways of BBR in rats were depicted in Fig. 7.

Among the obtained metabolites, M1 and M3 containing catechol structure were comparable to the detection of McDonald et al. [14]. They found that the metabolites containing catechol structure could combine with glutathione *in vitro*, furthermore, they guessed the metabolites likewise would combine with cysteine on the cell

membrane *in vivo*, which would induce the rupture of liver cells, leading to the toxicity of BBR. Unfortunately, we did not obtain the conjugates *in vivo* maybe due to their trace amount, the unsuitable selection of biological samples or the differences in species between humans and rats. All the questions need more in-depth study to be done.

4. Conclusions

Identity confirmation of chemicals using a TOF analyzer is well recognized and the results obtained in this study with the HPLC–QTOF-MS system confirmed the high-resolution capacity of this technique. Especially, the distinction between the loss of an oxygen atom and methane reflected the advantage of the QTOF instrument.

In conclusion, a fast, economic and accurate method was developed by HPLC–QTOF-MS system for detection of BBR metabolites in rats. The present results were found comparable to the literature data and thereby validated the reliability of our method for systematic studies on the biotransformation of BBR *in vivo*. Additionally, two reduced phase I metabolites and sets of phase II metabolites—sulfate adducts detected in our work were rarely reported in the literature. This study will help enhance the current knowledge of metabolism of BBR, and hopefully will urge us to advance in recognition of liver toxicity caused by BBR. Furthermore, the work is deemed to supply a reference to the cleavage rules of compounds by ESI-QTOF in negative mode.

Acknowledgement

The authors would like to gratefully acknowledge teacher Wu for her work on the word correction.

References

[1] G.M. McDonld, E. Allan Rettic, Chem. Res. Toxicol. 20 (2007) 1833.
[2] Y. Takahashi, K. Okuda, Clin. J. Gastroenterol. 10 (1993) 337.
[3] M.M. Van der Klauw, P.M. Houtman, B.H. Stricker, P. Spoeistra, J. Hepatol. 20 (1994) 376.
[4] M.L. Hautekeete, J. Henrion, S. Naegels, A. Deneve, M. Adler, C. Deprez, Liver 15 (1995) 25.
[5] P. Kaufman, M. Török, A. Hänni, R. Gasser, S. Krähenbühl, Clin. Pharmacol. Toxicol. 9 (2004) 27.
[6] J. Broekhuysen, M. Pacco, R. Sion, L. Demeulenaere, M. Van Hee, Eur. J. Clin. Pharmacol. 4 (1972) 125.
[7] H. Ferber, H. Vergin, G. Hitzenberger, Eur. J. Clin. Pharmacol. 19 (1981) 431.
[8] I. Walter-Sack, J.X. de Vries, A. Ittensohn, M. Kohlmeier, E. Weber, Klin. Wochenschr. 66 (1988) 160.
[9] P.J. Arnold, R. Guserle, V. Luckow, J. Chromatogr. 544 (1991) 267.
[10] I. Walter-Sack, U. Gresser, M. Adian, I. Kamilli, A. Ittensohn, J.X. de Vries, E. Weber, N. Zöllner, Eur. J. Clin. Pharmacol. 39 (1990) 173.
[11] J.X. de Vries, I. Walter-Sack, A. Ittensohn, E. Weber, H. Empl, U. Gresser, N. Zöllner, Clin. Invest. 71 (1993) 947.
[12] I. Walter-Sack, M. Eichelbaum, J.X. de Vries, E. Weber, Klin. Wochenschr. 66 (1988) 1097.
[13] I. Walter-Sack, J.X. de Vries, A. Ittensohn, E. Weber, Eur. J. Clin. Pharmacol. 39 (1990) 577.
[14] N.Z. Öllner, U. Gresser, I. Walter-Sack, Klin. Wochenschr. 68 (1990) 101.
[15] S.M. Ni, D.W. Qian, J.A. Duan, J.M. Guo, E.X. Shang, Y. Shu, C.F. Xue, J. Chromatogr. B 878 (2010) 2741.
[16] G.G. Tan, Z.Y. Lou, X. Dong, W.H. Li, W.T. Liao, Z.Y. Zhu, Y.F. Chai, J. Chromatogr. 74 (2011) 341.
[17] H.S. Lee, T.C. Jeong, J.H. Kim, J. Chromatogr. B 705 (1998) 367.
[18] R.F. Staack, J. Fehn, H.H. Maurer, J. Chromatogr. B 789 (2003) 27.
[19] E. Lyris, G. Tsiakatouras, Y. Angelis, M. Koupparis, M.H. Spyridaki, C. Georgakopoulos, J. Chromatogr. B 827 (2005) 199.